

Accepted Manuscript

Synthesis, characterization and DNA binding studies of two Ru(II) complexes containing guanidinium ligands

Wen-Xiu Chen, Xing-Dong Song, Jia-Xi Chen, Xuan-Hao Zhao, Jie-Hua Xing, Jun-Rui Ren, Tie Wu, Jing Sun

PII: S0277-5387(16)00132-7
DOI: <http://dx.doi.org/10.1016/j.poly.2016.02.038>
Reference: POLY 11854

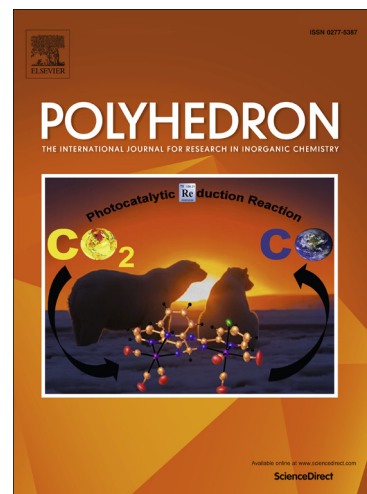
To appear in: *Polyhedron*

Received Date: 23 December 2015

Accepted Date: 16 February 2016

Please cite this article as: W-X. Chen, X-D. Song, J-X. Chen, X-H. Zhao, J-H. Xing, J-R. Ren, T. Wu, J. Sun, Synthesis, characterization and DNA binding studies of two Ru(II) complexes containing guanidinium ligands, *Polyhedron* (2016), doi: <http://dx.doi.org/10.1016/j.poly.2016.02.038>

This is a PDF file of an unedited manuscript that has been accepted for publication. As a service to our customers we are providing this early version of the manuscript. The manuscript will undergo copyediting, typesetting, and review of the resulting proof before it is published in its final form. Please note that during the production process errors may be discovered which could affect the content, and all legal disclaimers that apply to the journal pertain.



**Synthesis, characterization and DNA binding studies of two Ru(II)
complexes containing guanidinium ligands**

Wen-Xiu Chen^{†a}, Xing-Dong Song^{†a}, Jia-Xi Chen^{*a}, Xuan-Hao Zhao^a, Jie-Hua Xing^a, Jun-Rui Ren^a
Tie Wu^a, Jing Sun^{ab*}

^a *School of Pharmacy, Guangdong Medical University, Dongguan, 523808, China*

^b *Guangdong Key Laboratory for Research and Development of Natural Drugs, Guangdong Medical University, Zhanjiang, 524023, China*

[†] Contributed equally to this work.

^{*} Corresponding author. Tel.: +86-769-2289-6322; E-mail address: sunjing03@foxmail.com (Jing Sun);
cppcc@qq.com (Jia-Xi Chen).

Abstract

Two new Ru(II) complexes containing guanidinium groups have been synthesized, characterized and analyzed according to their interactions with different G-quadruplexes and duplex DNA. A FRET assay and a competitive FRET assay showed that both complexes promote the formation and stabilization of the human telomeric (h-telo) G-quadruplex and exhibit higher selectivity compared to promoters (such as c-myc, c-kit and bcl2) or duplex DNA. After binding to G-quadruplex, the two complexes have shown different DNA affinity and fluorescence enhancement. CD analyses further indicate that the two complexes display the ability to induce and stabilize the formation of antiparallel G-quadruplex structures in K^+ , Na^+ or ion-free buffers. The binding stoichiometry with h-telo was of the order of three ruthenium complexes per quadruplex.

Keywords: Synthesis; Ru(II) complex; G-quadruplex DNA; Guanidinium; H-telo

1. Introduction

It is well known that nucleic acid sequences rich in guanine (G) can form a special class of DNA structures known as G-quadruplexes (G4). These structures are comprised of a stack of G-tetrads, which are four guanines connected to each other through Hoogsteen hydrogen bonds to form a square planar structure [1-3]. Higher-ordered DNA structures are found in human telomeres (h-telo) and the promoter regions of many oncogenes, such as c-myc, c-kit and bcl2, and are guanine-rich. Telomerase is an enzyme present in over 85-90% of tumor cells, but it is not found in most normal cells [4,5]. This ribonucleoprotein increases the length of telomeres by adding polynucleotides to the ends, causing normal cells to divide uncontrollably and thus become tumor cells. Results show that the telomerase activity or oncogene expression, which are closely related to apoptosis, cellular proliferation and tumorigenesis [6,7], could be directly inhibited by the formation and stabilization of G-quadruplex structures. Moreover, the variety of the G-quadruplex DNA (G4-DNA) topological structures is different from duplex DNA, which further emphasizes that telomerase is an ideal probe for tumor diagnosis and a target for antitumor research [8,9]. It is crucial to find new compounds that are able to selectively interfere with the h-telo expression by the formation/stabilization of specific structures. Previous studies reported that G-quadruplex binders are organic compounds, and a number of metal complexes interact effectively with this DNA secondary structure [10-14]. The relative ease of the synthesis and the ability to vary the ligands and interchange the metal center increase the advantages of using metal complexes over their organic counterparts.

Successful quadruplex DNA binders should not only interact strongly with their target but also exhibit high selectivity for quadruplex DNA versus duplex DNA. The guanidinium group, the positively charged residues of arginine, plays a key role in many biological activities, such as molecular recognition and catalysis [15,16]. Meanwhile, the added positive charge increases the

non-specific binding of the metal-peptide conjugate due to electrostatic association with the negatively charged DNA backbone [17-19]. In this paper, we report the synthesis and characterization of G-quadruplex DNA binding of two new ruthenium(II) complexes (Scheme 1), $[\text{Ru}(\text{bpy})_2\text{L}^1]^{3-}$ (complex **1**) and $[\text{Ru}(\text{bpy})_2\text{L}^2]^{3+}$ (complex **2**) using 2,2-bipyridine (bpy), 1-(4-(1H-imidazo[4,5-f][1,10]phenanthrolin-2-yl)phenyl)guanidine hydrochloride (L^1) and 1-(3-(1H-imidazo[4,5-f][1,10]phenanthrolin-2-yl)phenyl)guanidine hydrochloride (L^2). Both structures proved to exhibit higher selectivity than promoters and duplex DNA. The obtained results will hopefully be of value for the future synthesis of Ru(II) complexes as potent telomerase inhibitors and also set a foundation for the rational design of new cancer chemotherapy drugs.

2. Materials and methods

2.1. Materials

DNA oligomers of 5'-AG₃[T₂AG₃]₃-3' DNA (h-telo), the fluorescent labelled oligonucleotide employed FRET probes: h-telo (5'-FAM-AG₃[T₂AG₃]₃-TAMRA-3', FAM = 6-carboxyfluorescein, TAMRA = 6-carboxy-tetramethylrhodamine), three promoter sequences c-myc (5'-FAM-[TG₄AGGGTGGGGAGGGTGGGGAAGG]-TAMRA-3'); c-kit (5'-FAM-[CGGGCGGGCGCGAGGGAGGGG]-TAMRA-3'); bcl2 (5'-FAM-[AGGGGCGGGCGCGGAGGAAGGGGGCGGGAGCGGGGCTG]-TAMRA-3') and a duplex DNA sequence F10T (5'-FAM-[TATAGCTATA-HEG-TATAGCTATA]-TAMRA-3' (the HEG linker is [(-CH₂-CH₂-O)₆]) were obtained from the Sangon Biotechnology Company. CT-DNA (calf thymus DNA) was purchased from the Sigma Company. Other reagents and solvents were commercially available. Four buffers were used in this work. Buffer A: 60 mM potassium cacodylate, pH 7.4; Buffer B: 100 mM KCl, 10 mM Tris, pH 7.4; Buffer C: 100 mM NaCl, 10 mM Tris, pH 7.4; Buffer D: 10 mM Tris, pH 7.4.

2.2. Physical measurements

Microanalysis (C, H and N) was carried out with a Perkin-Elmer 240C elemental analyzer. ^1H NMR spectra were recorded on a Varian Mercury-plus 300 NMR spectrometer with $(\text{CD}_3)_2\text{SO}$ and CD_3CN as solvents and SiMe_4 as an internal standard at 300 MHz at room temperature. Electrospray mass spectra (ESI-MS) were performed on an LQC system (Finngan MAT, USA). UV-Vis spectra were recorded on a Varian Cary 300 spectrophotometer. Emission spectra were recorded on a Perkin-Elmer Lambda-850 spectrophotometer and an Ls55 spectrofluorophotometer.

2.3. Preparation of the ligands and complexes

1,10-Phenanthroline-5,6-dione [20], 4-(1*H*-imidazo[4,5-*f*][1,10]phenanthrolin-2-yl)aniline, 3-(1*H*-imidazo[4,5-*f*][1,10]phenanthrolin-2-yl)aniline [21] and *cis*-[Ru(bpy) $_2$ Cl $_2$] \cdot 2H $_2$ O [22] were synthesized according to the methods reported in the referred literature.

2.3.1 Synthesis of 1-(4-(1*H*-imidazo[4,5-*f*][1,10]phenanthrolin-2-yl)phenyl)guanidine hydrochloride ($\text{L}^1\cdot\text{HCl}$)

A mixture of 4-(1*H*-imidazo[4,5-*f*][1,10]phenanthrolin-2-yl)aniline (0.4 g, 1.3 mmol) was completely dissolved in methanol (12 mL) and hydrochloric acid (1.5 mL) with stirring for 30 min. Next 50% cyanamide (4 mL) was added and refluxed for 20 h with the pH < 3. The solution was cooled to room temperature. After filtration, the yellow compound obtained was washed with cool ethanol and dried in a vacuum. Yield: 0.32 g (58.2%). Anal. Calcd for $\text{C}_{20}\text{H}_{16}\text{ClN}_7\cdot 2\text{H}_2\text{O}$ (425.87): C, 56.41; H, 4.73; N, 23.02. Found: C, 56.43; H, 4.72; N, 23.04%. ESI-MS, m/z : 354.2 [$\text{M}+\text{H}^+$] $^+$ (100), 707.0 [$2\text{M}+\text{H}^+$] $^+$ (10). ^1H NMR ($(\text{CD}_3)_2\text{SO}$) δ (ppm): 10.38 (s, H $_1$); 9.17 (dd, 2H); 8.57 (d, 2H); 8.20 (dd, 2H); 7.78 (s, 4H); 7.46 (t, 3H); 7.30 (s, H); 7.17 (s, 1H).

2.3.2 Synthesis of 1-(3-(1*H*-imidazo[4,5-*f*][1,10]phenanthrolin-2-yl)phenyl)guanidine hydrochloride ($\text{L}^2\cdot\text{HCl}$)

A mixture of 3-(1*H*-imidazo[4,5-*f*][1,10]phenanthrolin-2-yl)aniline (0.4 g, 1.3 mmol) was completely dissolved in methanol (12 mL) and hydrochloric acid (1.5 mL) with stirring for 30 min.

Next 50% cyanamide (4 mL) was added and refluxed for 48 h with the pH < 3. Upon cooling, a pink precipitate was obtained by dropwise addition of saturated aqueous Na₂CO₃ solution. The product was washed with H₂O until the pH was 7.0. The solid was then dissolved in 5 mL hydrochloric acid (3 M) and refluxed for 30 min; a pink compound was obtained after the solution was evaporated. Yield: 0.36 g (65.5%). Anal. Calcd for C₂₀H₁₆ClN₇·2H₂O (425.87): C, 56.41; H, 4.73; N, 23.02. Found: C, 56.40; H, 4.75; N, 23.05%. ESI-MS, m/z: 354.5 [M+H⁺]⁺ (100), 176.0 [M+2H⁺]²⁺ (20). ¹H NMR (CD₃CN) δ (ppm): 10.24 (s, H); 9.63 (d, 2H); 9.19 (d, 2H); 8.45 (d, H); 8.34 (s, H); 8.27 (dd, 2H); 7.68 (t, 5H); 7.41 (d, 1H).

2.3.3 [Ru(bpy)₂L¹](HPF₆)(PF₆)₂ (1)

Cis-Ru(bpy)₂Cl₂·2H₂O 0.14 g (0.26 mmol) and L¹ 0.11 g (0.26 mmol) were added to 20 mL ethanol-water (9:1, v/v). The mixture was refluxed for 2 h under the protection of argon. Upon cooling, a red complex was obtained after the addition of ammonium hexafluorophosphate. The crude product was purified by reversed-phase HPLC. Yield: 0.14 g (43.3%). Anal. Calcd for C₄₀H₃₂F₁₈N₁₁P₃Ru·2H₂O (1238.75): C, 38.78; H, 2.93; N, 12.44. Found: C, 38.76; H, 2.90; N, 12.47%. ESI-MS, m/z: 456 [M-2PF₆⁻]²⁺ (12), 383 [M-HPF₆-2PF₆⁻]²⁺ (31), 256 [M-3PF₆⁻]³⁺ (100). ¹H NMR (CD₃CN) δ (ppm): 9.12 (d, 2H); 8.62 (dd, 4H); 8.50 (d, 2H); 8.20 (t, 2H); 8.14 (d, 2H); 8.12 (d, 2H); 7.96 (d, 2H); 7.91 (dd, 3H); 7.70 (d, 2H); 7.62 (d, 2H); 7.57 (t, 3H); 7.34 (t, 3H); 6.47 (s, 3H). UV-Vis ((λ (nm), ε (M⁻¹ cm⁻¹)) (H₂O): 457 (12100), 283 (78300).

2.3.4 [Ru(bpy)₂L²](HPF₆)(PF₆)₂ (2)

This complex was obtained in an identical manner to that described for complex 1. L² (0.11 g, 0.26 mmol) was used in place of L¹. Yield: 0.15 g (47.3%). Anal. Calcd for C₄₀H₃₂F₁₈N₁₁P₃Ru·2H₂O (1220.73): C, 39.36; H, 2.81; N, 12.62. Found: C, 39.35; H, 2.84; N, 12.60%. ESI-MS, m/z: 1057 [M-PF₆⁻]⁺ (2), 456 [M-2PF₆⁻]²⁺ (28), 383 [M-HPF₆-2PF₆⁻]²⁺ (63), 256 [M-3PF₆⁻]³⁺ (100). ¹H NMR (CD₃CN) δ (ppm): 9.12 (d, 2H); 8.62 (dd, 5H); 8.40 (d, 1H); 8.32 (s,

1H); 8.22 (t, 3H); 8.14 (d, 2H); 8.12 (d, 2H); 7.97 (d, 3H); 7.91 (dd, 3H); 7.85 (d, 1H); 7.72 (d, 2H); 7.58 (m, 4H); 7.33 (t, 3H). UV-Vis (λ (nm), ϵ ($M^{-1} \text{ cm}^{-1}$)) (H_2O): 457 (13900), 282 (87400).

2.4 FRET assay

A FRET melting point assay was used to investigate the ability of the Ru(II) complexes to stabilize the different G-quadruplexes. Fluorescence melting curves were determined by a Roche Light Cycler II real-time PCR machine. The fluorescent labelled DNA was monitored alone and in the presence of the complexes in buffer A. The total reaction volume was 20 μL with 200 nM of the labelled oligonucleotide and different concentrations of the complexes (0, 1 and 2 μM). Measurements were made on a RT-PCR with excitation at 470 nm and detection at 530 nm. Fluorescence readings were taken at intervals of 1 $^{\circ}\text{C}$ from 37-99 $^{\circ}\text{C}$ with a constant temperature being maintained for 30 s prior to each reading to ensure the sample had reached equilibrium. T_m is the mid-point of a melting curve at which the complex is 50% dissociated.

The competition FRET-melting assay was similar to the FRET melting point assay, except different concentrations of duplex CT-DNA were added. This experiment was carried out to explore the selectivity of the Ru(II) complexes between h-telo DNA and duplex DNA.

2.5 Absorption and emission spectra

Absorption and emission titrations were carried out using 3 mL solutions of complexes **1** and **2** (10 μM , in buffer B) at room temperature, to which increments of the h-telo DNA stock solution were added. The Ru(II)-DNA solutions were allowed to incubate for 5 min before the spectra were recorded. The intrinsic binding constant K_b of the Ru(II) complex to DNA was calculated based on equations (1a) and (1b), which was applied to absorption titration data for non-cooperative metallointercalators binding to DNA [23-26], where [DNA] is the DNA concentration in base pairs. ϵ_a , ϵ_f , and ϵ_b correspond to the extinction coefficient ($A_{\text{abs}}/[M]$) observed for the MLCT absorption band at a given DNA concentration, the extinction coefficients for the free Ru(II) complex and

Ru(II) complex in the fully bound form, respectively. K_b is the equilibrium binding constant (M^{-1}); C_t is the total metal complex concentration and s is the binding site size.

$$(\varepsilon_a - \varepsilon_f)/(\varepsilon_b - \varepsilon_f) = (b - (b^2 - 2K_b^2 C_t [DNA]/s)^{1/2})/2K_b C_t \quad (1a)$$

$$b = 1 + K_b C_t + K_b [DNA]/2s \quad (1b)$$

2.6 Circular dichroism studies

Circular dichroism (CD) studies were used to observe the effect of the complexes on the structure of the h-telo DNA; these were performed on a JASCO J-810 spectropolarimeter at room temperature. Spectral data were collected from 200 to 350 nm with a scanning speed of 500 nm min^{-1} , scanning three times for each CD spectrum. The oligomers were re-suspended in buffers B, C and D. CD spectra were baseline-corrected for signal contributions due to the buffers. The CD titration was then performed at a constant DNA concentration (3 μM) with various concentrations of the complexes. All solutions were mixed thoroughly and allowed to equilibrate for 5 min before data collection.

2.7 Continuous Variation Analysis

The binding stoichiometries were obtained for the two complexes and h-telo according to the method of various proportions [27,28]. The mole fractions of the Ru(II) complex and DNA were varied from 0 to 1 in 0.1 increments in Buffer B, while the sum of the concentrations was kept at 10 μM . Each solution was equilibrated at 4 $^\circ\text{C}$ for 12 h with no light. The fluorescence intensities of these mixtures were measured at room temperature using an excitation wavelength of 458 nm for the two complexes. The F_{max} (fluorescence) was collected in the range 500-750 nm. The resulting curves show a break point at the molar fraction according to the binding stoichiometry of the complex.

3. Results and discussion

The synthetic route for the complexes is summarized in Scheme 1. Each synthetic step involved

here is straight forward and provides a moderate yield of the desired product in the pure form. These products were characterized by elemental analysis, ^1H NMR, ESI-MS and UV-Vis spectroscopy. The absorption spectra of the two Ru(II) complexes in water are characterized by a metal to ligand charge transfer (MLCT) in the visible region, at 457 nm, and an intense ligand-centered transition (LC) in the UV region, around 282 nm, typical of polypyridyl ruthenium(II) complexes [28,29]. The visible bands at 457 nm are attributed to the overlap of $\text{Ru}(\text{d}\pi) \rightarrow \text{bpy}(\pi^*)$ and $\text{Ru}(\text{d}\pi) \rightarrow \text{L}^1$ or L^2 (π^*) transitions. The ultraviolet bands around 282 nm for the two complexes can be attributed to (bpy) $\pi \rightarrow \pi^*$ transitions for $[\text{Ru}(\text{bpy})_2\text{L}]^{3+}$ [29].

(Scheme 1.)

FRET studies were used to investigate the thermodynamic stability of the two complexes to h-telo, promoter G-quadruplex DNA sequences (c-myc, c-kit and bcl2) and a duplex DNA sequence F10T. The ΔT_m values represent the increase in melting temperature between the initial DNA and DNA after addition of the Ru(II) complexes and representing the ability of the Ru(II) complexes to stabilize the different DNA. Reliable FRET melting curves (Figure 1) and ΔT_m values (Table 1) were obtained [30]. As shown in Table 1, the two complexes exhibit selectivity to h-telo G-quadruplex DNA at different concentrations. Both complexes had ΔT_m values > 23 °C with h-telo G-quadruplex; in contrast, the two complexes had ΔT_m values < 9 °C with c-myc, ΔT_m values < 18 °C with c-kit, ΔT_m values < 8 °C with bcl2 and ΔT_m values < 11 °C with duplex DNA at 2 μM . At the same time, the two Ru(II) complexes displayed high ΔT_m values with h-telo G-quadruplex of 22.5 and 19.2 °C ($[\text{Ru}]/[\text{DNA}] = 5/1$) for **1** and **2** respectively, which were higher than that of the complex $[\text{Ru}(\text{bpy})_2(\text{dppz})]^{2+}$ (4.7 °C, $[\text{Ru}]/[\text{DNA}] = 1/1$) [25], but smaller than that of the complex $[\text{Ru}(\text{bpy})_2(\text{ptpn})]^{2+}$ (26 °C, $[\text{Ru}]/[\text{DNA}] = 5/1$) [11]. Although most of the ΔT_m values observed for complex **2** were smaller than those for complex **1** in K^+ buffer, the results suggest that the two Ru(II) complexes are good h-telo G-quadruplex stabilizers.

(Figure 1.)

(Table 1.)

In addition to the high stabilization ability, the two Ru(II) complexes also exhibited high selectivity for quadruplex DNA over duplex DNA. The DNA competition FRET-melting assay was carried out to show the ΔT_m change for 2.0 μM of the Ru(II) complexes with 200 nM h-telo by adding varying concentrations of the double-stranded CT-DNA in K^+ buffer [31]. Figure 2 shows the melting point change with 2.0 μM Ru(II) complexes by adding CT-DNA in buffer A. As shown in Table 2, the ΔT_m values do not change significantly, even though the CT-DNA is present at a concentration 50 times that of h-telo, showing duplex DNA has a negligible effect on the binding of ligands to G-quadruplex DNA. The above results indicate that both the Ru(II) complexes not only have a high stabilization ability, they also have better selectivity for h-telo DNA.

(Figure 2.)

(Table 2.)

Absorption titration spectra were performed to determine the binding affinity of the complexes with h-telo. The electronic spectral traces of the complexes titrated with DNA are shown in Figure 3. The data of the UV absorption titration with DNA for complexes **1** and **2** are listed in Table 3. Upon addition of h-telo, the MLCT transition bands of the two complexes exhibit different degrees of hypochromism and red shifting changes. There is a significant difference in the DNA-binding intrinsic constants. The intrinsic binding constants, K_b , of the two complexes **1** and **2** in K^+ buffer were respectively $(1.37 \pm 0.09) \times 10^6$ and $(1.08 \pm 0.80) \times 10^5 \text{ M}^{-1}$, in which complex **1** is much greater and has a stronger DNA-binding affinity than complex **2**. The results obtained by absorption spectra titrations overall are consistent with those obtained by the FRET assay. The two complexes have the same ancillary ligand (bpy). The difference in DNA affinity ability mostly originates from the difference between the intercalative ligands, which can be explained by the lower steric

hindrance of L^1 in complex **1** than that of L^2 in complex **2**. In general, a larger steric hindrance in the intercalative ligand will reduce the interaction of the complexes with DNA.

(Figure 3.)

(Table 3.)

Luminescence titration measurements were used to further clarify the nature of the interaction between the complexes and h-telo DNA. Figure 4 displays the results of the luminescence titration for the two complexes with h-telo. Upon excitation using a wavelength of 458 nm, both complexes exhibit luminescence in buffer B with a maximum wavelength at about 600 nm. The luminescence intensity of the complexes increases with an increase in the DNA concentration and reaches a maximum at a ratio of $[DNA]/[Ru] \approx 13:1$, at which there is a 2.44 and 2.19-fold increase in the fluorescence intensity for complexes **1** and **2**, respectively. The binding constants of the two complexes interacting with DNA from the emission spectra were obtained using the luminescence titration method [32]. The binding data obtained from the emission spectra were fitted using the McGhee-von Hippel equation [33] to acquire the binding parameters. The intrinsic binding constants K_b of $1.44(\pm 0.23) \times 10^6 M^{-1}$ for complex **1** and $9.84(\pm 0.98) \times 10^5 M^{-1}$ for complex **2** were determined. Although the binding constants obtained from fluorescence spectra with the McGhee-von Hippel method are different from those obtained from absorption spectra, both sets of binding constants show that complex **1** binds to DNA more avidly than complex **2**.

(Figure 4.)

CD spectroscopy was employed to characterize the solution formation of h-telo G-quadruplex induced by Ru(II) complex. It has been reported that h-telo G-quadruplexes generally consist of a mixed conformation (parallel/antiparallel) in K^+ solution [34-36]. The CD spectrum showed a large positive band around 290 nm, a small positive band at 250 nm and a negative band at 235 nm. In the presence of Na^+ ions, the CD spectrum had a 295 nm positive band and a 265 nm negative band,

which may be characteristic of an antiparallel G-quartet structure [37,38]. The CD spectrum of the h-telo sequence indicated the coexistence of a single strand and two types of quadruplex structures, parallel and antiparallel G-quadruplexes, in the absence of metal cations [34,39,40].

As shown in Figure 5(a), upon addition of the two complexes, dramatic changes in the CD spectra were observed. The maximum at 290 nm was gradually suppressed, and two positive bands at 281 and 295 nm increased. At the same time, the positive band at 248 nm was gradually suppressed and a major negative band at 260 nm started to appear. It seemed that in the presence of the complexes, the mixed parallel G-quadruplex decreased, forming an antiparallel G-quadruplex instead, and the CD signal at 281 nm may be induced through the strong absorbance of the two complexes at about 285 nm (Figure 3) [41]. In Na⁺ solution, the intensity of the bands at 260 nm increased on addition of the two Ru(II) complexes, while a minor shoulder positive band at about 280 nm was observed, and the intensity of the band centered at 295 nm increased significantly [Figure 5(b)]. These changes suggest that the two Ru(II) complexes can further stabilize the antiparallel G-quadruplex structure. In the ion-free system, the CD spectrum of h-telo consists of a small negative band at 240 nm, a major positive band at 255 nm, and a rather broad and small positive signal around 295 nm. Addition of the complexes increased the CD intensity of the band at 295 nm and decreased the band at 255 nm; the negative band at 260 nm began to appear and gradually increased [Figure 5(c)]. This is typical for the antiparallel G-quadruplex structure as described above. All of the results imply that the two complexes can induce h-telo into an antiparallel G-quadruplex structure and stabilize it even at high metal strength.

(Figure 5.)

A luminescence-based Job plot was used to determine the stoichiometry interactions between the complexes and h-telo DNA. From the intersection points obtained in Figure 6, binding stoichiometries for complexes **1** and **2** in K⁺ buffer were obtained. The Ru(II) complexes

demonstrated binding stoichiometries of the order of three ruthenium complexes per G-quadruplex.

(Figure 6.)

Small molecules can potentially bind to a quadruplex by externally stacking below the quartets, intercalating between the quartets, or non-specifically binding to some random location on the DNA strand [41,42]. The most important interaction between G-quartets and the octahedral Ru(II) complexes in solution is thought to partially stack on or intercalate the G-tetrads [43]. Given the CD results, the structure of the two complexes and the positive charge of the metal ion, the main mode of interaction is thought to occur through the intercalative mode. Meanwhile, the guanidinium groups with the cationic charge probably give rise to an additional interaction with the negatively charged phosphate backbones of DNA through hydrogen-bonding and electrostatic interactions [19,44]. Detailed investigations on the binding modes and the biological activity are in progress.

4. Conclusion

In summary, two new Ru(II) complexes, $[\text{Ru}(\text{bpy})_2\text{L}]^{3+}$, containing guanidinium ligands have been synthesized and characterized. Both complexes show good selectivity for h-telo G-quadruplex compared to promoters and duplex DNA. The results of absorption and emission titrations indicate that complex **1** has a greater DNA affinity than complex **2**. The 3:1 stoichiometry suggests that three complexes molecules interact with one molecule of G-quadruplex DNA. Given the CD spectra, we propose that the Ru(II) complexes most likely interact with h-telo DNA through the intercalative mode.

Appendix A. Supplementary data

Nine figures (Figure S1-9) for ESI-MS spectra of L^1 , L^2 , **1** and **2**, ^1H NMR spectra of L^1 , L^2 , **1** and **2**, and UV-Vis spectra of **1** and **2**, respectively.

Acknowledgments

We are grateful to the National Natural Science Foundation of China (21101034), the Yong Teachers Training Plan of Guangdong Province (Yq2013086), the Science and Technology Plan of Dongguan City (2011108102046) and the innovative items for undergraduates of Guangdong Province (201510571038).

References

- [1] M. Gellert, M.N. Lipsett, D.R. Davies, *Proc. Natl. Acad. Sci. U. S. A.* 48 (1962) 2013.
- [2] J.T. Davis, *Angew. Chem., Int. Ed.* 43 (2004) 668.
- [3] J.L. Huppert, *Chem. Soc. Rev.* 37 (2008) 1375.
- [4] N.W. Kim, M.A. Piatyszek, K.R. Prowse, C.B. Harley, M.D. West, P.L. Ho, G.M. Coviello, W.E. Wright, S.L. Weinrich, J.W. Shay, *Science* 266 (1994) 2011.
- [5] L.R. Kelland, *Anticancer Drugs* 11 (2000) 503.
- [6] K. Suntharalingam, D. Gupta, P.J.S. Miguel, B. Lippert, R. Vilar, *Chem. Eur. J.* 16 (2010) 3613.
- [7] T. Finkel, M. Serrano, M.A. Blasco, *Nature* 448 (2007) 767.
- [8] A.M. Burger, F. Dai, C.M. Schultes, A.P. Reszka, M.J. Moore, J.A. Double, S. Neidle, *Cancer Res.* 65 (2005) 1489.
- [9] V. Gabelica, E. Shammel Baker, M.P. Teulade-Fichou, E. De Pauw, M.T. Bowers, *J. Am. Chem. Soc.* 129 (2007) 895.
- [10] S.N. Georgiades, N.H.A. Karim, K. Suntharalingam, R. Vilar, *Angew. Chem. Int. Ed.* 49 (2010) 4020.
- [11] X. Chen, J.H. Wu, Y.W. Lai, R. Zhao, H. Chao, L.N. Ji, *Dalton Trans.* 42 (2013) 4386.
- [12] X.H. Zheng, Q. Cao, Y.L. Ding, Y.F. Zhong, G. Mu, P.Z. Qin, L.N. Ji, Z.W. Mao, *Dalton Trans.* 44 (2015) 50.
- [13] S. Shi, X. Gao, H.L. Huang, J. Zhao, T.M. Yao, *Chem. Eur. J.* 21 (2015) 13390.
- [14] X. Gao, S. Shi, J.L. Yao, J. Zhao, T.M. Yao, *Dalton Trans.* 44 (2015) 19264.

- [15] S.L. Tobey, E.V. Anslyn, *J. Am. Chem. Soc.* 125 (2003) 14807.
- [16] H. Fu, Y.H. Zhou, W.L. Chen, Z.G. Deqing, M.L. Tong, L.N. Ji, Z.W. Mao, *J. Am. Chem. Soc.* 128 (2006) 4924.
- [17] J. Brunner, J.K. Barton, *Biochemistry* 45 (2006) 12295.
- [18] C.A. Puckett, J.K. Barton, *Bioorg. Med. Chem.* 18 (2010) 3564.
- [19] J. He, J. Sun, Z.W. Mao, L.N. Ji, H.Z. Sun, *J. Inorg. Biochem.* 103 (2009) 851.
- [20] W. Paw, R. Eisenberg, *Inorg. Chem.* 36 (1997) 2287.
- [21] Y.J. Liu, C.H. Zeng, H.L. Huang, L.X. He, F.H. Wu, *Eur. J. Med. Chem.* 45 (2010) 564.
- [22] B.P. Sullivan, D.J. Salmon, T.J. Meyer, *Inorg. Chem.* 17 (1978) 3334.
- [23] M.T. Carter, M. Rodriguez, A.J. Bard, *J. Am. Chem. Soc.* 111 (1989) 8901.
- [24] P.U. Maheswari, M. Palaniandavar, *J. Inorg. Biochem.* 98 (2004) 219.
- [25] S. Shi, X.T. Geng, J. Zhao, T.M. Yao, C.R. Wang, D.J. Yang, L.F. Zheng, L.N. Ji, *Biochimie* 92 (2010) 370.
- [26] I. Haq, P. Lincoln, D. Suh, B. Norden, B.Z. Chowdhry, J.B. Chaires, *J. Am. Chem. Soc.* 117 (1995) 4788.
- [27] I. Haq, J.O. Trent, B.Z. Chowdhry, T.C. Jenkins, *J. Am. Chem. Soc.* 121 (1999) 1768.
- [28] H. Deng, J.W. Cai, H. Xu, H. Zhang, L.N. Ji, *J. Chem. Soc., Dalton Trans.* (2003) 325.
- [29] S. Shi, T. Xie, T.M. Yao, C.R. Wang, X.T. Geng, D.J. Yang, L.J. Han, L.N. Ji, *Polyhedron* 28 (2009) 1355.
- [30] J.L. Mergny, J.C. Maurizot, *ChemBioChem* 2 (2001) 124.
- [31] A. Arola-Arnal, J. Benet-Buchholz, S. Neidle, R. Vilar, *Inorg. Chem.* 47 (2008) 11910.
- [32] S. Satyanarayana, J.C. Dabrowiak, J.B. Chaires, *Biochemistry* 31 (1992) 9319.
- [33] J.D. McGhee, P. H. Von Hippel, *J. Mol. Biol.* 86 (1974) 469.
- [34] E.M. Rezler, J. Seenisamy, S. Bashyam, M.Y. Kim, E. White, W.D. Wilson, L.H. Hurley, J.

Am. Chem. Soc. 127 (2005) 9439.

[35] A. Ambrus, D. Chen, J.X. Dai, T. Bialis, R.A. Jones, D. Yang, *Nucleic Acids Res.* 34 (2006) 2723.

[36] Y. Xu, Y. Noguchi, H. Sugiyama, *Bioorg. Med. Chem.* 14 (2006) 5584.

[37] C. Antonacci, J.B. Chaires, R.D. Sheardy, *Biochemistry* 46 (2007) 4654.

[38] J. Dai, C. Punchihewa, A. Ambrus, D. Chen, R.A. Jones, D. Yang, *Nucleic Acids Res.* 35 (2007) 2440.

[39] P. Balagurumoorthy, S.K. Brahmachari, D. Mohanty, M. Bansal, V. Sasisekharan, *Nucleic Acids Res.* 20 (1992) 4061.

[40] W. Li, P. Wu, T. Ohmichi, N. Sugimoto, *FEBS Lett.* 526 (2002) 77.

[41] S. Shi, J. Liu, T.M. Yao, X.T. Geng, L.F. Jiang, Q.Y. Yang, L. Cheng, L.N. Ji, *Inorg. Chem.* 47 (2008) 2910.

[42] E.S. Baker, J.T. Lee, J. L. Sessler, M.T. Bowers, *J. Am. Chem. Soc.* 128 (2006) 2641.

[43] C. Rajput, R. Rutkaite, L. Swanson, I. Haq, J.A. Thomas, *Chem. Eur. J.* 12 (2006) 4611.

[44] H.X. Sun, Y.L. Tang, J.F. Xiang, G.Z. Xu, Y.Z. Zhang, H. Zhang, L.L. Xu, *Bioorg. Med. Chem. Lett.* 16 (2006) 3586.

Table 1. The effect of complexes **1** and **2** on the T_m of h-telo, c-myc, c-kit, bcl2 and duplex DNA

F10T determined from FRET ([DNA] = 200 nM)

	h-telo	c-myc	c-kit	bcl2	F10T
Complex	$\Delta T_m(^{\circ}\text{C})$				
1 (2 uM)	25.74	8.80	17.80	2.60	9.60
1 (1 uM)	22.54	5.20	14.00	0.26	4.60
2 (2 uM)	23.20	6.94	16.39	7.40	10.50
2 (1 uM)	19.20	6.14	9.00	5.20	8.26

Table 2. The effect of complexes **1** and **2** on the T_m of h-telo DNA ([DNA] = 200 nM)

Complex	h-telo	h-telo+2 uM Ru(II)	h-telo+2 uM Ru(II) +5 uM CT-DNA	h-telo+2 uM Ru(II) +10 uM CT-DNA
	T_m (°C)	ΔT_m (°C)		
1	51.34	27.03	27.43	29.00
2	51.34	23.40	23.63	23.80

ACCEPTED MANUSCRIPT

Table 3. Absorption spectra (λ_{\max}/nm) and DNA-binding constants K_b (M^{-1}) of complexes **1** and **2**

Complex	$\lambda_{\max}(\text{free})$	$\lambda_{\max}(\text{bound})$	$\Delta\lambda/\text{nm}$	H/(%)	K_b/M^{-1}	s
1	457	460	3	32.63	$1.37\pm 0.9(\times 10^6)$	0.24 \pm 0.04
	285	289	4	40.48		
2	458	463	5	18.19	$1.08\pm 0.8(\times 10^5)$	0.025 \pm 0.02
	284	287	3	19.16		

ACCEPTED MANUSCRIPT

Scheme and Figure Captions

Scheme 1. Synthetic routes for the preparation of the ligands L^1 and L^2 , and the complexes **1** and **2**.

Figure 1. FRET-melting curves for experiments carried out in buffer A (60 mM potassium cacodylate, pH 7.4) with h-telo, c-myc, c-kit, bcl2 and duplex DNA F10T separately with the two complexes **1** and **2**; [DNA] = 200 nM.

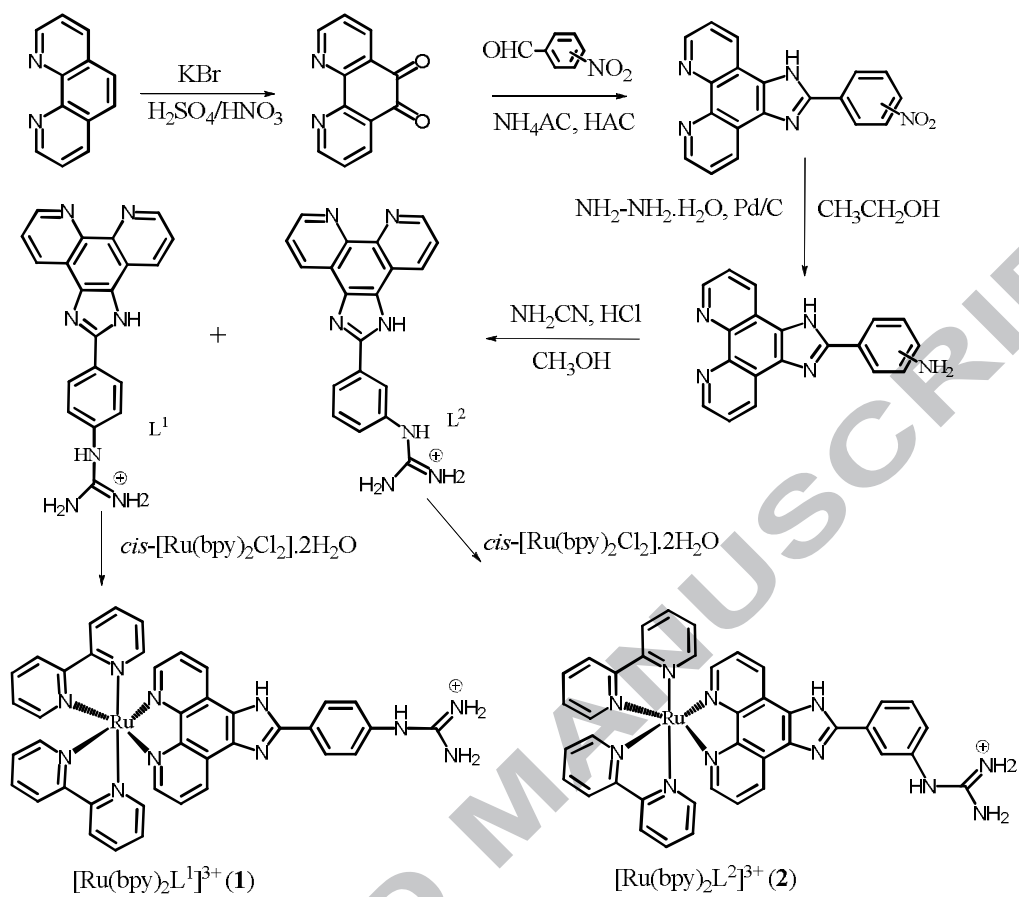
Figure 2. FRET competition experiments of the complexes **1** and **2** at 2 μ M concentration showing the h-telo DNA (200 nM) melting temperature with different concentration of CT-DNA in buffer A (60 mM potassium cacodylate, pH 7.4).

Figure 3. Absorption spectra of complexes **1** and **2** in buffer B (100 mM KCl, 10 mM Tris, pH 7.4) with increasing amounts of h-telo DNA; [Ru] = 10 μ M, [DNA] = 0-14 μ M from top to bottom. Arrows refer to the change in absorbance upon increasing the DNA concentration. Inset: plot of $(\epsilon_a - \epsilon_f)/(\epsilon_b - \epsilon_f)$ vs. [DNA] and the non-linear fit for the titration of DNA to Ru(II) complexes.

Figure 4. Emission spectra of complexes **1** and **2** in buffer B (100 mM KCl, 10 mM Tris, pH 7.4) with increasing amounts of h-telo DNA; [Ru] = 10 μ M, [DNA] = 0-14 μ M. Arrow refers to the emission intensity changes upon increasing DNA concentrations.

Figure 5. CD spectra of G-quadruplex induced by complexes **1** and **2** with 3 μ mol L^{-1} h-telo at room temperature. (a) **1** and **2** in a buffer of 100 mM KCl, 10 mM Tris, pH 7.4; (b) **1** and **2** in a buffer of 100 mM NaCl, 10 mM Tris, pH 7.4; (c) **1** and **2** in a buffer of 100 mM NaCl, 10 mM Tris, pH 7.4. Arrows indicate the increasing amounts of complexes. $r = 0 \sim 6$ ($r = [Ru]/[DNA]$)

Figure 6. Job plot using luminescence data for complexes **1** (■) and **2** (●) with a final G-quadruplex at 10.0 μ M in buffer solution of 100 mM KCl, 10 mM Tris, pH 7.4.



Scheme 1

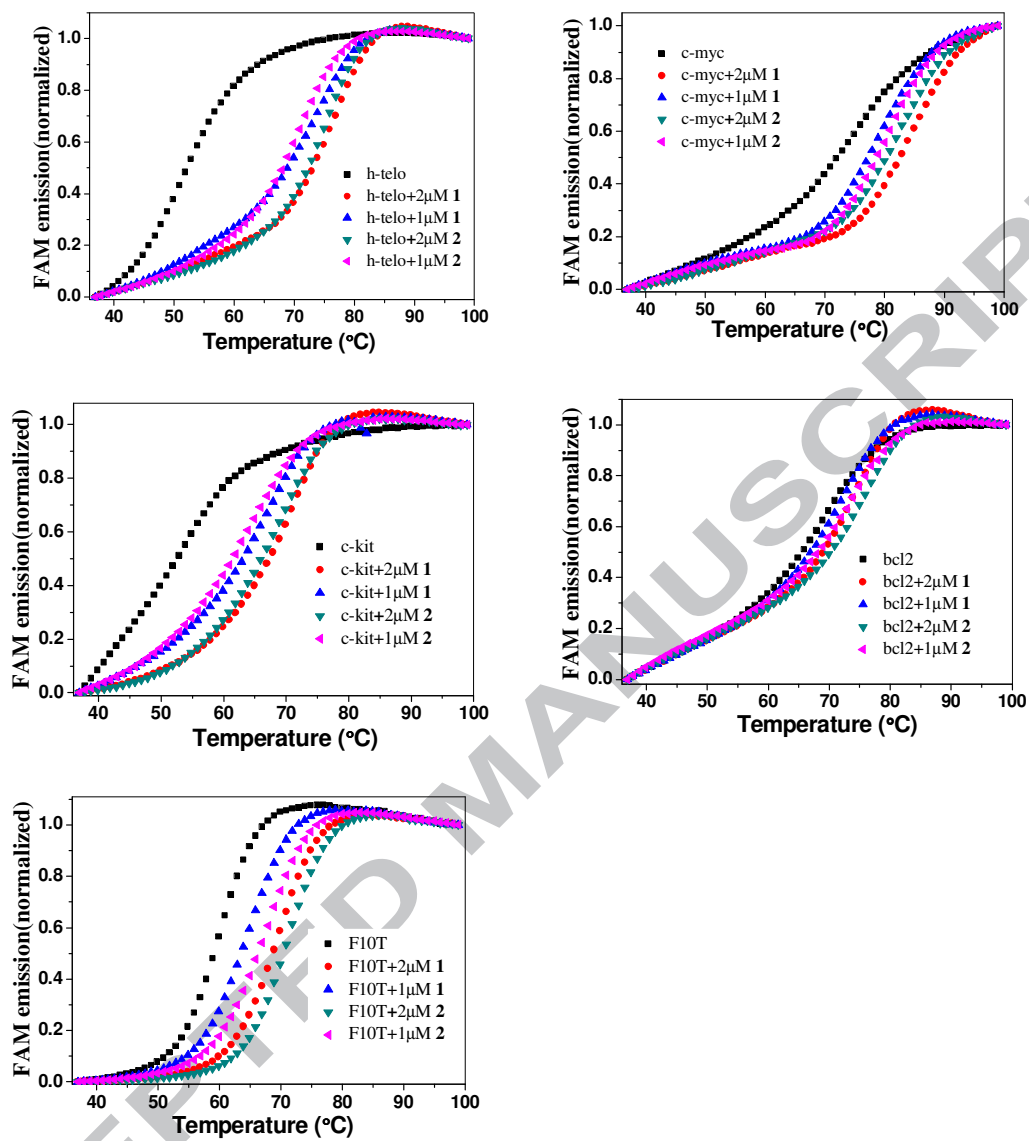


Figure 1.

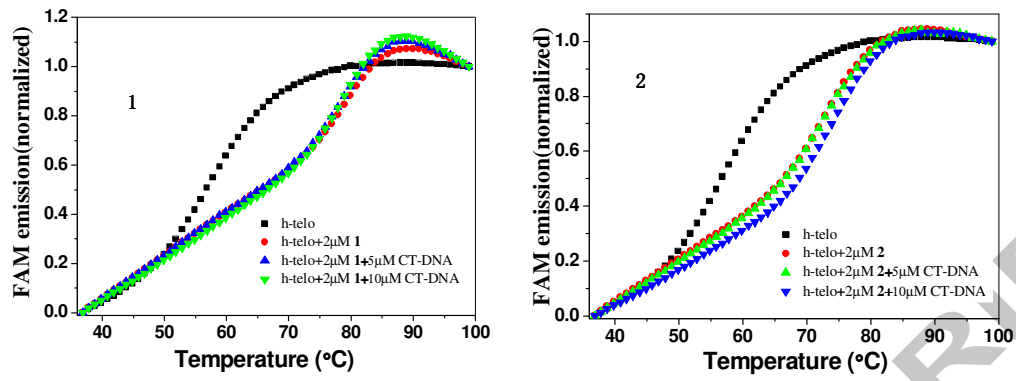


Figure 2.

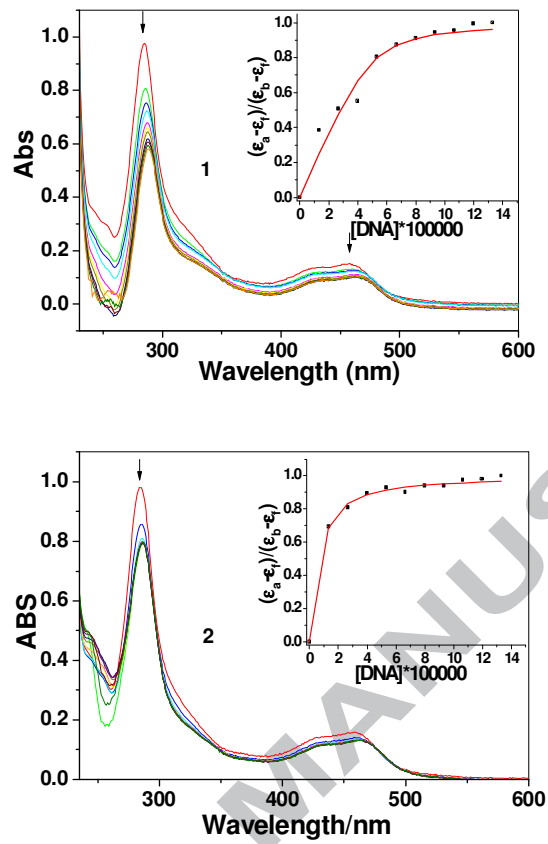


Figure 3.

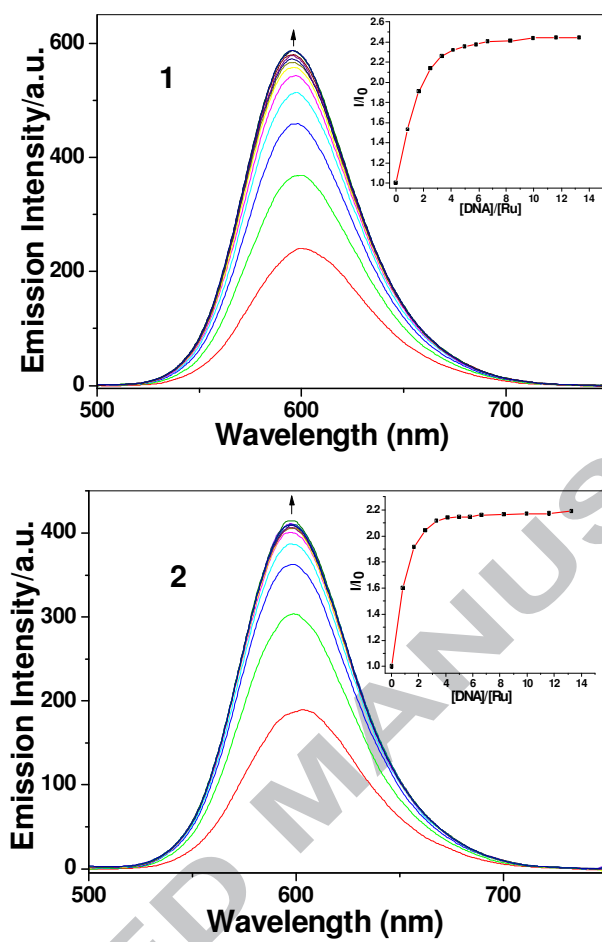


Figure 4.

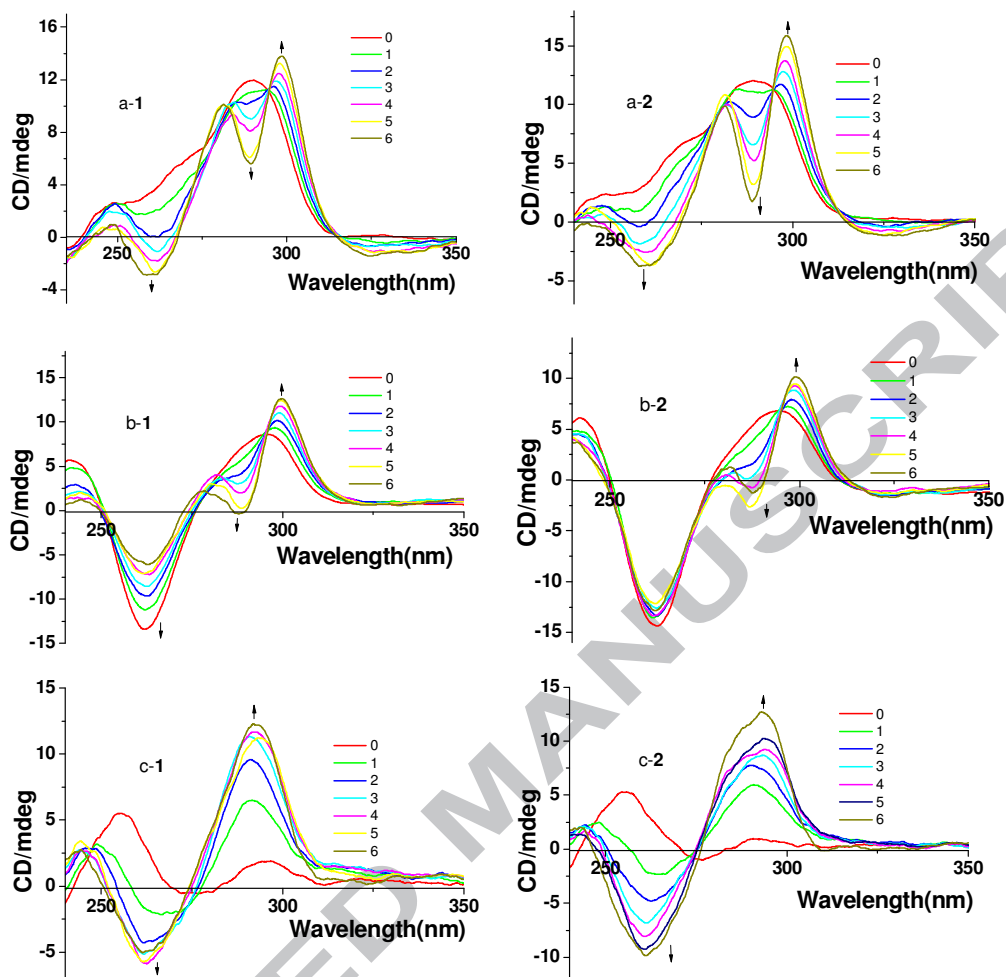


Figure 5.

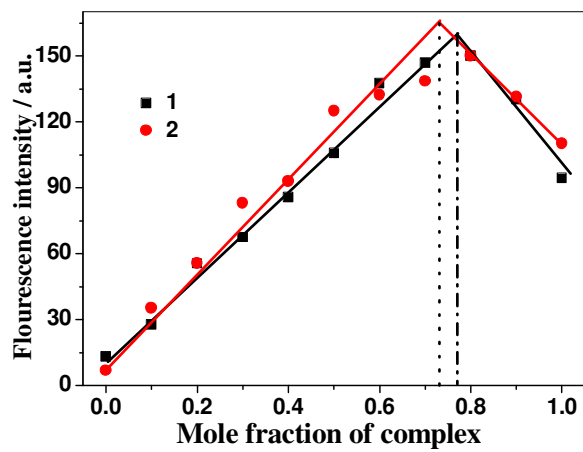
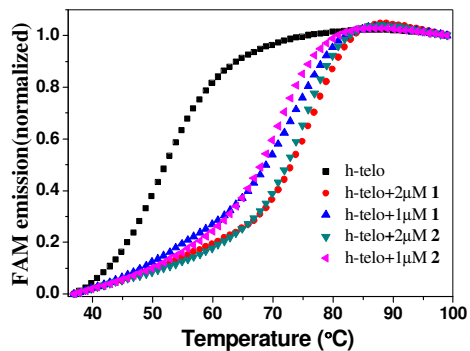


Figure 6.

ACCEPTED MANUSCRIPT



Synthesis, characterization and DNA binding studies of two Ru(II) complexes containing guanidinium ligands

Wen-Xiu Chen, Xing-Dong Song, Jia-Xi Chen, Xuan-Hao Zhao, Jie-hua Xing, Jun-Rui Ren, Tie Wu, Jing Sun

Two new Ru(II) complexes, $[\text{Ru}(\text{bpy})_2\text{L}]^{3+}$ (**1** and **2**), containing guanidinium ligands have been synthesized and characterized. Both complexes show good selectivity for h-telo G-quadruplex DNA compared to promoters and duplex DNA.